

*Engen E. Lundquist*

# NATIONAL ADVISORY COMMITTEE FOR AERONAUTICS

TECHNICAL MEMORANDUM

No. 1164

PRESSURE-DISTRIBUTION MEASUREMENTS ON  
UNYAWED SWEEPED-BACK WINGS

By W. Jacobs

Translation

“Druckverteilungsmessungen an Pfeilflügeln konstanter  
Tiefe bei symmetrischer Anströmung”

Deutsche Luftfahrtforschung, Untersuchungen und Mitteilungen Nr. 2052



Washington

July 1947



## NATIONAL ADVISORY COMMITTEE FOR AERONAUTICS

## TECHNICAL MEMORANDUM No. 1164

PRESSURE-DISTRIBUTION MEASUREMENTS ON  
UNYAWED SWEEPED-BACK WINGS\*

By W. Jacobs

## SYNOPSIS

This report presents comprehensive pressure-distribution measurements on four (4) swept-back wings ( $\phi = 0^\circ, 15^\circ, 30^\circ$ , and  $45^\circ$ ) of constant chord and over a large range of angles of attack with symmetrical air flow. The distributions, experimentally obtained, were compared with theoretical ones calculated by the methods of Weissinger and Multhopp.

## I. INTRODUCTION

Because of the ever increasing importance of swept-back wings at high speeds the question of the load distribution on the wing becomes more and more in need of an exact answer. The answer here can only be given by pressure-distribution measurements. It is important to have a systematic series of measurements so as to bring out the influence of sweepback angle and minimize that of the airfoil profile. Heretofore only little experimental data was obtained. Some of this data was run on half-span wings and the end-plate effect thoroughly falsified the true effect of sweepback. The data for the straight wing (that is, no sweepback) have already been presented by Möller.

## II. NOTATION AND RELATIONS

$x, y$  coordinates fixed to the airplane;  $\xi = \frac{2x}{b}$ ;  $\eta = \frac{2y}{b}$   
 $\xi, \eta$  dimensionless coordinates

---

\*"Druckverteilungsmessungen an Pfeilflügeln konstanter Tiefe bei symmetrischer Anströmung." Zentrale für wissenschaftliches Berichtswesen der Luftfahrtforschung des Generalluftzeugmeisters (ZWB) - Berlin-Adlershof, Untersuchungen und Mitteilungen Nr. 2052, Braunschweig, Dec. 21, 1943.

F	wing area
b	wing span
l	wing chord
$\Lambda$	wing aspect ratio
$\phi$	wing sweepback angle
$\alpha$	angle of attack measured from wing chord
$y_s$	distance from the lift center point of a wing-half to the symmetry plane
$y_{sR}$	distance from the load center of a winghalf to the symmetry plane
$\Delta y_s$	shift of the load center because of sweepback
$x_N$	shift of the neutral point compared to the zero sweepback wing
$x_N'$	distance from the neutral point to area centroid
$(x_N')_R$	shift in neutral point of the sweepback wing with the lift distribution of $\phi = 0^\circ$ wing
$\Delta x_N'$	shift in neutral point of the arrow wing following the change in lift distribution as against the $\phi = 0$ wing (fig. 4)

Moment reference axis: Axis through 1/4 pt. of profile section through wing centroid of one winghalf.

### III. WIND-TUNNEL MODELS.

Four (4) wings were used,  $\phi = 0^\circ, 15^\circ, 30^\circ,$  and  $45^\circ$  (fig. 1). They all have the same chord parallel to the body center line and have the same aspect ratio = 5.18. Profile NACA 23012 was chosen. Swept-back wings were obtained from the straight wing by shearing parallel to the symmetry plane. Wing tips were provided with a rounded tip having a radius equal to half of the local wing thickness. Twist and dihedral were not provided.

Wing dimensions

$$\begin{aligned}
 b &= 0.770 \text{ m} \\
 l &= 0.150 \text{ m} \\
 F &= 0.1146 \text{ m}^2 \\
 A &= 5.18
 \end{aligned}$$

English units

$$\begin{aligned}
 b &= 30.3 \text{ in.} \\
 c &= 5.9 \text{ in.} \\
 S &= 177.7 \text{ sq in.} \\
 A.R. &= 5.18
 \end{aligned}$$

The wings were constructed in the usual way of steel spars and brass ribs. The ribs were reinforced and provided with lightening holes. The measuring slots were distributed in such a way as to secure an optimum lift distribution; therefore, they had to be closer to each other at the wing tips than at the center of the wing. The total number of the slots for wings with the sweepback  $\phi = 0^\circ$  and  $\phi = 15^\circ$  was 15; 16 slots were selected for wings with  $\phi = 30^\circ$  and  $\phi = 45^\circ$ . Twelve and thirteen slots, respectively, were located on one-half wing. The rest was added to guarantee the lift distribution at the center of the wing. Figure 1 shows the exact position of the slots. Nineteen holes were provided for chordwise pressure measurements; their position also is given in figure 1. All slots at equal distance from the front edge were connected by a narrow brass tube; the tube was led out at the side averted from the half of measurement. All the small tubing could then be guided out of the jet stream in a main tube to a multiple-tubed manometer. The connections of the single tubes were attached underneath the surface so that a reliable force test could be carried out after the main tube has been removed. The areas between the ribs of the rectangular wing and the swept-back wing  $\phi = 15^\circ$  consisted of brass plate. In the wings with  $30^\circ$  and  $45^\circ$  sweepback they had been filled out with plaster. In both cases the wing support was adequate.

## IV. CARRYING OUT THE OBSERVATIONS; RESULTS

Measurements were taken in the wind tunnel of the Aerodynamic Institute of the Advanced Technological School of Braunschweig. At an airspeed  $v = 40$  meters per second (90 mph) the Reynolds number was  $vl/\nu = 4.2 \times 10^5$ . When the measurements on 1 chord were taken the slots of all other chords were closed with cellophane. For each observation an airtightness test was made. The angles of attack that were used are:

$$\alpha = -3.9^\circ, 1.9^\circ, 5.7^\circ, 8.5^\circ, 11.4^\circ, 14.4^\circ$$

Before making the pressure tests, force tests were made. The results of the three-component tests are given in figure 2. The moments are referred to the axis through the 1/4 chord point at the centroid of the half-wing area. From the measurements the following was derived:

#### A. Three-Component Measurements

The lift-curve slope  $\frac{\partial c_a^1}{\partial \alpha}$  decreases somewhat with sweepback, slowly at first, it is true, but quite markedly at  $45^\circ$  sweepback. (See fig. 3, table 1.)  $c_{a_{max}}$  increases up to  $\phi = 30^\circ$  and then decreases. Whether the Reynolds number plays a role here cannot be determined, although other measurements show similar behavior (11). From theory only an increase of  $c_{a_{max}}$  was to be expected (that is, for increasing  $\phi$ ) because lift at small  $\phi$ 's is more evenly distributed over the wing. In American measurements (8), carried out at considerably higher Reynolds numbers, this increase is not observable.

At low  $c_a$  values the drag is about the same for all wings, as can be seen from the polars. It is only at the higher  $c_a$  values that the drag increases with sweepback angle. This increase is not caused, first of all, by the induced drag; otherwise, an increase in profile drag is to be charged to the outer part of the wing as was shown in a previous investigation (7) of impulse measurements along the wing span. This drag increase is caused by the concentration of the boundary-layer material on the outside of the wing because of secondary currents in the boundary layer.

The position of the neutral point or the moment slope  $\partial c_M / \partial c_a$  is shown in table 1. Here the reference axis is the axis through the centroid of the half wing. In what follows we shall give the general expression for the neutral point as a consequence of the sweepback angle. We introduce the following terminology (fig. 4). (See II.) It then follows from figure 4:

---

<sup>1</sup> $c_a$  is the German equivalent of the English  $C_L$

$$y_s = y_{sR} + \Delta y_s$$

$$x_N = \frac{b}{4} \tan \phi - x_{N'} = y_s \tan \phi$$

$$x_N = \frac{b}{4} \tan \phi - (x_{N'})_R + \Delta x_{N'}$$

$$x_{N'} = (x_{N'})_R - \Delta x_{N'}$$

$$x_{N'} = \left( \frac{b}{4} - y_s \right) \tan \phi = \left( \frac{b}{4} - y_{sR} - \Delta y_s \right) \tan \phi$$

$$(x_{N'})_R = \left( \frac{b}{4} - y_{sR} \right) \tan \phi$$

$$\Delta x_{N'} = \Delta y_s \tan \phi$$

Written dimensionlessly:

$$\frac{(x_{N'})_R}{l} = \left( \frac{1}{2} - \frac{y_{sR}}{b/2} \right) \tan \phi \frac{\Lambda}{2} \quad (1)$$

$$\frac{\Delta x_{N'}}{l} = \frac{\Delta y_s}{b/2} \frac{\Lambda}{2} \tan \phi \quad (2)$$

This quantity  $\Delta x_{N'}/l$  defines the neutral point shift because of the lift change of a swept-back wing as against a straight wing. This will therefore be critical, if in the calculation of the neutral point of a swept-back wing the lift distribution of the straight wing is taken as the starting point. The neutral point shift from the straight wing is given by:

$$\frac{x_N}{l} = \frac{b}{4l} \tan \phi - \frac{\Lambda}{2} \left( \frac{1}{2} - \frac{y_{sR}}{b/2} \right) \tan \phi + \frac{\Lambda}{2} \frac{\Delta y_s}{b/2} \tan \phi \quad (3)$$

In this equation the first term is the shift in neutral point that comes about from pushing back the wing area centroid (one-half wing) at constant  $c_{n_{local}}$  distribution; the second term gives the additional shift to account for the lift distribution of the straight wing deviating from the constant  $c_{n_{local}}$  distribution; the third term, finally, gives the further additional shift following from the difference in lift distribution between the swept-back wing and the straight wing.

### B. Pressure-Distribution Measurements

The results of the pressure-distribution measurements for the various wings are presented in figures 5, 6, 7, and 8. The normal-force coefficient is here plotted against the dimensionless span coefficient. From these plots one concludes that the wing lift distribution changes its nature with sweepback angle; indeed a displacement of the lift towards the wing tips shows up. While in the case of the straight wing (fig. 5) a continuous decrease in lift occurs as one goes out from the symmetry plane to the tips, the lift in the central section becomes so depressed in swept-back wings (with large  $\phi$ ), that an increase in lift is noticeable as one goes out toward the tip. (See figs. 7 and 8.) At a sweepback angle of  $45^\circ$ , this depression is present at all angles of attack. This has as a consequence, in the  $c_{e_{max}}$  region, that the separation moves outward with increasing sweepback angle. A few flow pictures show this effect very clearly on various wings. (See fig. 11.) While the flow on the straight wing, at a  $15^\circ$  angle of attack, first separates in the central section, separation on the  $15^\circ$  sweepback wing has already moved out towards the wing tips. On the  $30^\circ$  and  $45^\circ$  sweepback wings this trend is still more marked.

A comparison of the integrated lift forces from the pressure distributions with the force measurements shows that, considering the small shifts in zero lift, there is satisfactory agreement. (See fig. 3.) The values obtained from pressure measurements are somewhat smaller than those obtained from force measurements.

For the evaluation of longitudinal stability the location of the centroids of the lift distribution of a half wing is very important. Its distance to the symmetry plane of the wing  $y_s$  is obtained graphically from the measured lift distribution, if we form:

$$\frac{y_s}{b/2} = \frac{\int_0^1 c_n \eta \, d\eta}{\int_0^1 c_n \, d\eta}$$

The dependence of this lateral locus of the centroids of the swept-back configurations is seen in figure 10. Here is plotted the average for angles of attack of  $1.9^\circ$ ,  $5.7^\circ$ ,  $8.5^\circ$ , and  $11.4^\circ$ . The largest angle was omitted, for in this case separation toward the wing tips could falsify the picture. One sees the relations clearly, namely, that with increasing sweepback angle the center of gravity of the load moves outward. Compared with the straight wing this travel amounts to about 3 percent of the half span of the wing. This causes by equation (2), a neutral point shift:

$$\frac{\Delta x_N'}{l} = 0.08$$

that is, 8 percent of the wing chord, which surpasses the admissible difference by quite an amount. The lift values obtained from the pressure measurements of the straight wing must not be taken as characteristic under any circumstances in the calculation of the neutral point of a swept-back wing.

## V. COMPARISON OF EXPERIMENTAL AND THEORETICAL VALUES

We shall now make a comparison between the observed values and the values given by theory. For the calculation of the lift distribution there are three methods available:

(1) Multhopp's method (3). - This method starts from Prandtl lifting-line theory and adds correction factors.

(2) Lifting-surface method of Weissinger (5). - This method is based on a plane circulation distribution around the wing.

(3) Lifting-line method of Weissinger (5). - In this case the lifting line is again used. This line is located on the quarter chord line and the circulation distribution is so determined that the downwash induced by the vortex system on the three-quarter chord line is equal to the normal component of the relative wind.

The calculations based on the lifting surface are complicated and time consuming. The lifting-line method is essentially simpler. Weissinger has shown that in practice there is no difference between the two methods and that one may use the lifting-line method without any misgivings. Multhopp's method is the simpler of the two. It appears, however, when it comes to a comparison between theoretical and experimental values, that Multhopp's method is inferior to Weissinger's.

The lift distributions  $\gamma(\eta)$  for the various swept-back wings, calculated by the method of Multhopp and Weissinger, are shown in figure 9. In this figure  $\gamma(\eta)$  means  $\Gamma/bv$ . Multhopp's calculation is based on  $c_{a_{\infty}}' = \frac{2\pi}{3.20}$ , Weissinger's on  $c_{a_{\infty}}' = \frac{5.26}{2\pi}$ . In carrying out Multhopp's method the correction factor used was  $\kappa = 1$ . From a comparison between experimental and theoretical values the following holds:

(1) Lift increase. - Following Multhopp the proportionality factor between circulation and effective angle of attack is independent of sweepback angle, so that  $\partial c_a / \partial \alpha = \text{const}$ . The theory of the lifting surface, after Weissinger, yields a decrease in integrated lift and, therefore, of the lift change with increasing sweepback angles. The values of  $\partial c_a / \partial \alpha$  after Weissinger, are shown in figures 3 and 9. The measurements show a smaller decrease in  $\partial c_a / \partial \alpha$  than expected from the theoretical values and is indeed only 60 per cent of the theoretical value.

notified?  
change 4-9-51

(2) Lift distribution.- More important than the question of total lift is that of the lift distribution because this distribution is a determining factor in the position of the neutral point and in the separation behavior at high sweepback angles. A comparison between theoretical lift distribution and the ones calculated from the pressure distribution measurements is contained in figures 5, 6, 7, and 8. Here the distributions calculated after Weissinger and Multhopp are reduced based on the corresponding measured  $c_n$ -values, in that the theoretical curves are multiplied by a factor, so that the  $c_n$ -values correspond with those observed. As can be seen from figure 5, considerable discrepancy is already shown by the trend of the curves of the straight wing. The lift distribution after Multhopp is "fuller" than that after Weissinger. The theory of Weissinger yields undisputably a better agreement with measured pressure distributions than that of Multhopp. This difference can also be explained by the fact that the plane circulation distribution was not considered. It is also naturally contained in the calculation of lift distribution in the case of swept-back wings. Thereto should also be added other differences between the two methods. The comparison is contained in figures 6, 7, and 8. The lift distribution after Weissinger shows quite good agreement with experimental values at all sweepback angles. It is only at the center of the wing and sweep angles of  $30^\circ$  and  $45^\circ$  that large discrepancies occur. Theory here yields too small a value. At large angles of attack good agreement is not to be expected because of separation phenomena.

Multhopp's theory yields in all cases results inferior to those of Weissinger. From the measurements the displacement of the lift toward the tips with increasing sweep angle is not as pronounced as that given by Multhopp's theory. This becomes very clear when we compare the load centroids obtained from observation and theory. This is shown in figure 10. Here are plotted the observed lift centers averaged over  $\alpha = 1.9^\circ, 5.7^\circ, 8.5^\circ,$  and  $11.4^\circ$ . To avoid distorting the picture  $\alpha$ 's of  $-3.9^\circ$  and  $14.3^\circ$  were not used. Agreement with Weissinger's theory is very good. Multhopp's theory in all cases yields values that are too high. The results of force measurements, given for comparison's sake and previously published (7), show small differences from the

pressure-distribution measurements. This can be traced back to the fact that the moment curves are not rectilinear, and thus the derivative  $dc_M/dc_a$  contains a certain indeterminacy. (See fig. 2.) Furthermore, the often used average between rectangular and elliptical lift distributions is included. These distributions yield too large values for the load centroid for small sweep angles and too small values at large sweep angles. From this data an approximation is produced for obtaining the neutral point location, although for all sweep angles  $0 \leq \phi \leq 45$  the mistake is 0.02% at the most.

From the location of the lift centroid one can immediately determine the location of the neutral point, important in stability calculations and indeed we will only consider the change in position of neutral point caused only by the shift in load center point. This value is decisive because in the determination of the neutral point of a swept wing the lift distribution of the straight wing is used as a starting point. The magnitude of this shift is given by equation (2):

$$\frac{\Delta x_{N'}}{l} = \frac{\Delta y_s}{b/2} \frac{\Lambda}{2} \tan \phi. \quad \text{These values are given in table 6.}$$

From the pressure measurements it is seen that there is a shift of 7.8 percent of the wing chord between the straight wing and  $45^\circ$  sweepback wing. One can see that this value greatly exceeds the maximum tolerable shift, which in general should move in the neighborhood of 1 percent. At large sweepback angles one must allow for the change in the lift distribution.

In what follows we shall compare the neutral point locations for various theoretical lift distributions with force and pressure distribution measurements. This is done in table 7. The neutral point is here calculated from the quarter chord in the wing center, after figure 4. As next point, the constant  $c_{n_{local}}$  distribution will be taken up as the simplest case. The resulting neutral-point locations are identical with the aft position of the area centroid. The average between rectangular and elliptical lift distributions is also shown, being often used as an approximation. Further are shown neutral-point locations obtained by correcting to the swept-back wings the measured lift distributions of the straight wing. The newer results obtained from the

theory of Multhopp and Weissinger are also contained in table 7, 1, next to the experimental values calculated from force-and pressure-distribution measurements. If one requires an accuracy of 1 percent of the wing chord for the neutral-point location, then a comparison between theory and observation shows that such a requirement is fulfilled only by Weissinger's computation method. Multhopp's method yields a value quite too large. Fortunately, the average between rectangular and elliptical lift distributions yields only an error of about 2 percent, which in most cases is sufficient in large approximation calculations.

In table 7, 2 is contained the shift of the neutral point as a consequence of lift distribution deviation from the constant  $c_{a_{local}}$  distribution (I-I, 1).

Table 7,3 shows the influence of the change in lift distribution of the swept-back wing as against the straight wing.

Summarizing, we can on the basis of those results, establish that Weissinger's theory gives the best approximation to the observed values, as can be judged from figure 10 and tables 6 and 7. The difference in regard to the neutral-point location remains within 1 percent of the wing chord. Multhopp's theory yields too large a value for the load centroid and therefore also for the neutral-point location at high sweepback angles. In practice, it does not matter whether one uses Weissinger's method or the average of rectangular and elliptical distributions: Either one yields a good approximation. The error for sweepback angles  $0 \leq \varphi \leq 45^\circ$  remains within 2 percent of the wing chord.

## VI. SUMMARY

Weissinger's method is superior to Multhopp's.

Translated by W. J. Nemerever  
Curtiss-Wright Corporation

## VII. BIBLIOGRAPHY

1. Blenk, H.: Göttinger Sechskomponenten-Messungen an Flügeln mit V-Form, Pfeilform und Verwindung. DVL-Jahrbuch 1929, p. 133.
2. Multhopp, H.: Die Berechnung der Auftriebsverteilung von Tragflügeln. Luftfahrtforschung, Bd. 15 (1938).
3. Multhopp, H.: Die Anwendung der Tragflügeltheorie auf Fragen der Flugmechanik bei unsymmetrischer Anströmung. Bericht S 2 der Lilienthal-Gesellschaft für Luftfahrtforschung (1939).
4. Weissinger, J.: Der schiebende Tragflügel bei gesunder Strömung. Jahrbuch 1940 der deutschen Luftfahrtforschung, p. I 145.
5. Weissinger, J.: The Lift Distribution of Swept-Back Wings. NACA TM No. 1120, March 1947.
6. Schlichting, H.: Neuere Beiträge der Forschung zur aerodynamischen Flügelgestaltung (Umriss, Verwindung, Rumpfeinfluß). Jahrbuch 1940 der deutschen Luftfahrtforschung, p. I 115.
7. Jacobs, W.: Sechskomponentenmessungen an drei Pfeilflügeln. FB 1629 (1942).
8. Andersen: The Experimental and Calculated Characteristics of 22 Tapered Wings. NACA Rep. Nr. 572, 1936.
9. Moller, E.: Sechskomponentenmessungen an Rechteckflügeln mit V-Form und Pfeilform in einem großen Schiebewinkelbereich. Lufo 1941, Lfg. 7, Bd. 18, p. 243.
10. Ludwig, H.: Pfeilflügel bei hohen Geschwindigkeiten. Bericht Nr. 127 der Lilienthal-Gesellschaft f. Luftfahrtforschung über die Sitzung "Hochgeschwindigkeit" in Braunschweig und Göttingen (Sept. 1940).
11. Hansen, M.: Tragflügel konstanter Tiefe mit Pfeilstellung und Verwindung beim Schieben. Forschungsbericht Nr. 1411 (1941).

12. Luetgebrune, H.: Beiträge zur Pfeilflügeluntersuchung.  
FB 1458.
13. Luetgebrune, H.: Druckverteilungsmessungen an  
Pfeilflügeln. FB 1501 (1941).
14. Göthert, R., and Scholkemeier: Sechskomponentenmessungen  
und Druckverteilungsmessungen an einem Rechteckflügel  
und einem Ellipsenflügel. FB 1451 (1941).
15. Möller, E.: Druckverteilungsmessungen an einem Hoch-  
und Tief-decker bei symmetrischer und unsymmetrischer  
Anströmung. Jahrbuch 1943 der deutschen Luft-  
fahrtforschung.

TABLE 1.- MOMENT CURVE AND LIFT-CURVE SLOPES, FROM FORCE MEASUREMENTS. REFERENCE POINT: QUARTER CHORD POINT OF THE PROFILE SECTION GOING THROUGH THE HALF-WING CENTROID

$\phi^\circ$	$\partial c_M / \partial c_a$	$\partial c_a / \partial \alpha$
0	0	3.89
15	.024	3.85
30	.051	3.62
45	.073	3.33

TABLE 2.- STRAIGHT WING  $\phi = 0^\circ$ . NORMAL-FORCE COEFFICIENTS  $c_{n_{local}}$ ; FROM PRESSURE-DISTRIBUTION MEASUREMENTS

Measuring cross section	$\alpha$ $\eta$	$-3.9^\circ$	$1.9^\circ$	$5.6^\circ$	$8.5^\circ$	$11.4^\circ$	$14.3^\circ$
		1	0.961	-0.074	0.046	0.194	0.353
2	.932	-.102	.060	.226	.362	.458	.649
3	.877	-.127	.094	.304	.469	.568	.744
4	.738	-.167	.148	.406	.577	.739	.906
5	.584	-.185	.180	.473	.667	.838	1.003
6	.487	-.193	.183	.500	.693	.875	1.068
7	.390	-.204	.192	.539	.714	.913	1.094
8	.292	-.199	.206	.560	.742	.938	1.128
9	.195	-.199	.216	.563	.755	.963	1.140
10	.097	-.203	.219	.568	.765	.975	1.149
11	.049	-.201	.216	.564	.765	.971	1.146
12	0	-.200	.215	.550	.772	.972	1.152
Average	$\bar{c}_n$	-0.175	0.164	0.460	0.647	0.818	1.007

TABLE 3.- SWEEPED-BACK WING  $\phi = 15^\circ$ . NORMAL-FORCE  
 COEFFICIENTS  $c_{n_{local}}$ ; FROM PRESSURE-  
 DISTRIBUTION MEASUREMENTS

Measuring cross section	$\alpha$		$-3.9^\circ$	$1.9^\circ$	$5.6^\circ$	$8.5^\circ$	$11.4^\circ$	$14.3^\circ$
	$\eta$							
1	0.961		-0.056	0.082	0.265	0.462	0.617	0.858
2	.932		-.065	.114	.269	.418	.652	.703
3	.877		-.129	.174	.355	.521	.642	.769
4	.738		-.138	.207	.457	.652	.803	.945
5	.584		-.173	.218	.525	.724	.885	1.038
6	.487		-.192	.234	.540	.750	.920	1.071
7	.390		-.193	.240	.550	.768	.940	1.093
8	.292		-.188	.240	.558		.952	1.104
9	.195		-.194	.240	.560	.770	.952	1.124
10	.097		-.203	.235	.547	.760	.958	1.135
11	.049		-.158	.242	.546	.758	.956	1.135
12	0		-.173		.552	.742	.961	1.138
13	-.049		-.177	.249	.546	.753	.953	1.120
14	-.097		-.199	.250	.542	.751	.960	1.103
15	-.195		-.175	.238	.591	.759	.968	1.108
Average	$\bar{c}_n$		-0.163	0.208	0.483	0.683	0.850	1.001

TABLE 4.- SWEEP-BACK WING  $\phi = 30^\circ$ . NORMAL-FORCE  
 COEFFICIENTS  $c_{n_{local}}$ ; FROM PRESSURE-  
 DISTRIBUTION MEASUREMENTS

Measuring cross section	$\alpha$		$-3.9^\circ$	$1.9^\circ$	$5.7^\circ$	$8.5^\circ$	$11.4^\circ$	$14.3^\circ$
	$\eta$	$c_n$						
1	0.963	-0.078	0.054	0.178	0.303	0.479	0.604	
2	.855	-.118	.058	.222	.318	.451	.499	
3	.896	-.130	.094	.285	.401	.516	.531	
4	.818					.626	.754	
5	.740	-.190	.157	.411	.566	.708	.805	
6	.584	-.223	.178	.448	.627	.793	.904	
7	.487	-.233	.172	.454	.638	.808	.943	
8	.390	-.241	.157	.450	.655	.825	.973	
9	.292	-.253	.154	.452	.663	.829	1.003	
10	.195	-.252	.138	.441	.651	.823	1.011	
11	.097	-.248	.153	.457	.646	.833	1.014	
12	0	-.275	.149	.451	.641	.847	1.018	
13		-.277	.156	.452	.641	.842	1.035	
14		-.255	.145	.456	.621	.828	.991	
15		-.097	.147	.444	.636	.819	1.025	
16		-.195	.150	.461	.645	.814	1.030	
Average	$\overline{c_n}$	-0.210	0.146	0.405	0.582	0.745	0.882	

TABLE 5.- SWEEPED-BACK WING  $\phi = 45^\circ$ . NORMAL-FORCE  
 COEFFICIENTS  $c_{n_{local}}$ ; FROM PRESSURE-  
 DISTRIBUTION MEASUREMENTS

Measuring cross section	$\alpha$ $\eta$	$-3.9^\circ$	$1.9^\circ$	$5.7^\circ$	$8.6^\circ$	$11.5^\circ$	$14.4^\circ$
		1	0.963	-0.076	0.0745	0.177	0.272
2	.935	-.093	.0934	.205	.293	.374	.532
3	.896	-.110	.125	.263	.369	.462	.551
4	.818	-.129	.152	.296	.421	.525	.627
5	.740	-.144	.178	.330	.450	.557	.691
6	.584	-.162	.179	.345	.471	.601	.750
7	.487	-.170	.178	.348	.490	.626	.774
8	.390	-.191	.180	.349	.490	.625	.800
9	.292	-.185	.159	.336	.486	.615	.799
10	.195	-.192	.146	.338	.478	.611	.785
11	.097		.137	.335		.603	.782
12	.049	-.201	.130	.325	.475	.601	.768
13	0	-.192	.132	.325	.463	.610	.745
14	-.049	-.185	.133	.337	.469	.608	.742
15	-.097	-.188	.138	.340	.482	.618	.755
16	-.195	-.183	.145	.349	.499	.640	.778
17	-.292	-.175	.151	.361	.511	.650	.815
Average	$\overline{c_n}$	-0.158	0.152	0.317	0.446	0.563	0.710

TABLE 6.- LOCATION OF THE LOAD CENTROID OF A HALF WING AND SHIFT IN NEUTRAL POINT CAUSED

BY A CHANGE OF THE LIFT DISTRIBUTION  $\left( \frac{\Delta x_N'}{l} = \frac{\Delta y_s}{b/2} \frac{\Lambda}{2} \tan \varphi \right)$ .

COMPARISON BETWEEN THEORY AND OBSERVATIONS

φ	Pressure-distribution measurements			Force measurements			Theory Weissinger (5)			Theory Muthopp (3)			Average of rectangular and elliptical lift distributions		
	$\frac{y_s}{b/2}$	$\frac{\Delta y_s}{b/2}$	$\frac{\Delta x_N'}{l}$	$\frac{y_s}{b/2}$	$\frac{\Delta y_s}{b/2}$	$\frac{\Delta x_N'}{l}$	$\frac{y_s}{b/2}$	$\frac{\Delta y_s}{b/2}$	$\frac{\Delta x_N'}{l}$	$\frac{-y_s}{b/2}$	$\frac{\Delta y_s}{b/2}$	$\frac{\Delta x_N'}{l}$	$\frac{y_s}{b/2}$	$\frac{\Delta y_s}{b/2}$	$\frac{\Delta x_N'}{l}$
0	0.442	0	0		---	---	0.438	0	0	0.450	0	0	0.465	0	0
15	.450	.008	.006	0.454	---	---	.448	.010	.007	.463	.013	.009	.465	0	0
30	.460	.018	.027	.462	---	---	.457	.019	.028	.477	.027	.040	.465	0	0
45	.473	.031	.078	.467	---	---	.472	.034	.088	.497	.047	.122	.465	0	0

TABLE 7: Comparison of theoretical and observed neutralpoint locations.  
 The value  $X_N/l$  ( $X_N$  is calculated from the quarterchord point in symmetry plane)

		Calculation					Observation	
$\psi^\circ$	① constant $C_n$ local distribution	② average of rectangular and elliptical distribution	③ corrected by means of the observed distribution of the straight wing	④ from Multhopp's theory	⑤ from Weissinger's theory	⑥ from force measurements	⑦ from pressure distribution measurements	
I	0	0	0	0	0	0	0	
	15	0,344	0,320	0,304	0,319	0,309	0,315	
	30	0,741	0,691	0,657	0,709	0,678	0,683	
	45	1,283	1,190	1,136	1,279	1,210	1,215	

The value  $\Delta X_N/l = 1-1$  ① : =

Shift in neutral point location as a consequence of the deviation of the lift distribution from a constant  $C_{nlocal}$ -distribution.

II	0	0	0	0	0	0	0
	15	-0,024	-0,040	-0,025	-0,035	-0,029	-0,034
	30	-0,050	-0,084	-0,032	-0,063	-0,051	-0,058
	45	-0,093	-0,147	-0,004	-0,073	-0,073	-0,068

The value  $\Delta X_N/l = 1-1$  ③ : =

Shift in neutral point in consequence of the deviation of the lift distribution from that of an unswept rectangular wing.

III	0	0		0	0	0	0
	15	0,040	0,016	0,015	0,005	0,011	0,006
	30	0,084	0,034	0,052	0,021	0,033	0,026
	45	0,147	0,054	0,143	0,074	0,074	0,079

Fig. 1

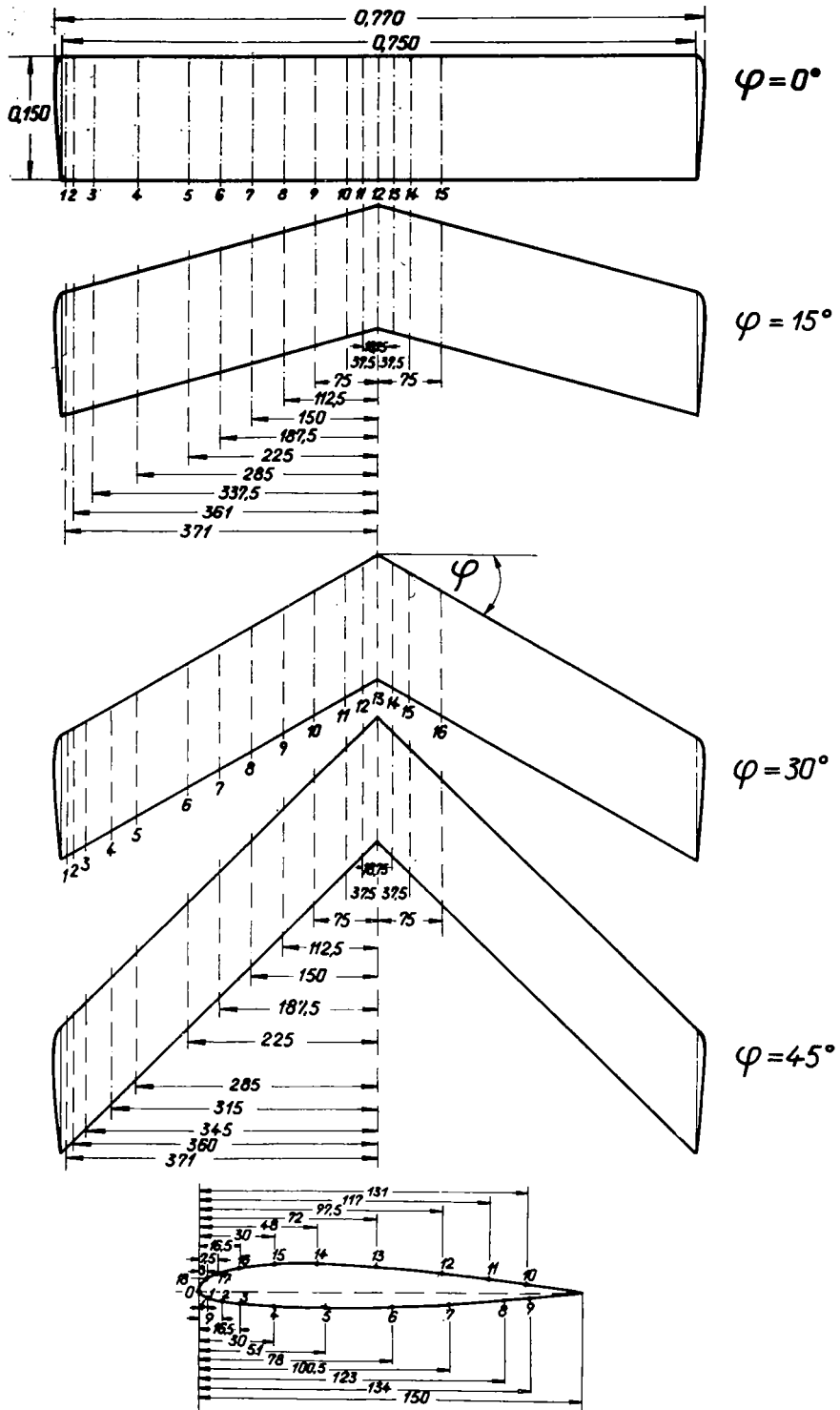


Figure 1.- Comparison between the utilized sweptback wings and location of measurement sections and holes.  $b = 0.770$  m;  $l = 0.150$  m;  $F = 0.1146$  m<sup>2</sup>;  $\Lambda = 5.18$ ; profile NACA 23012.

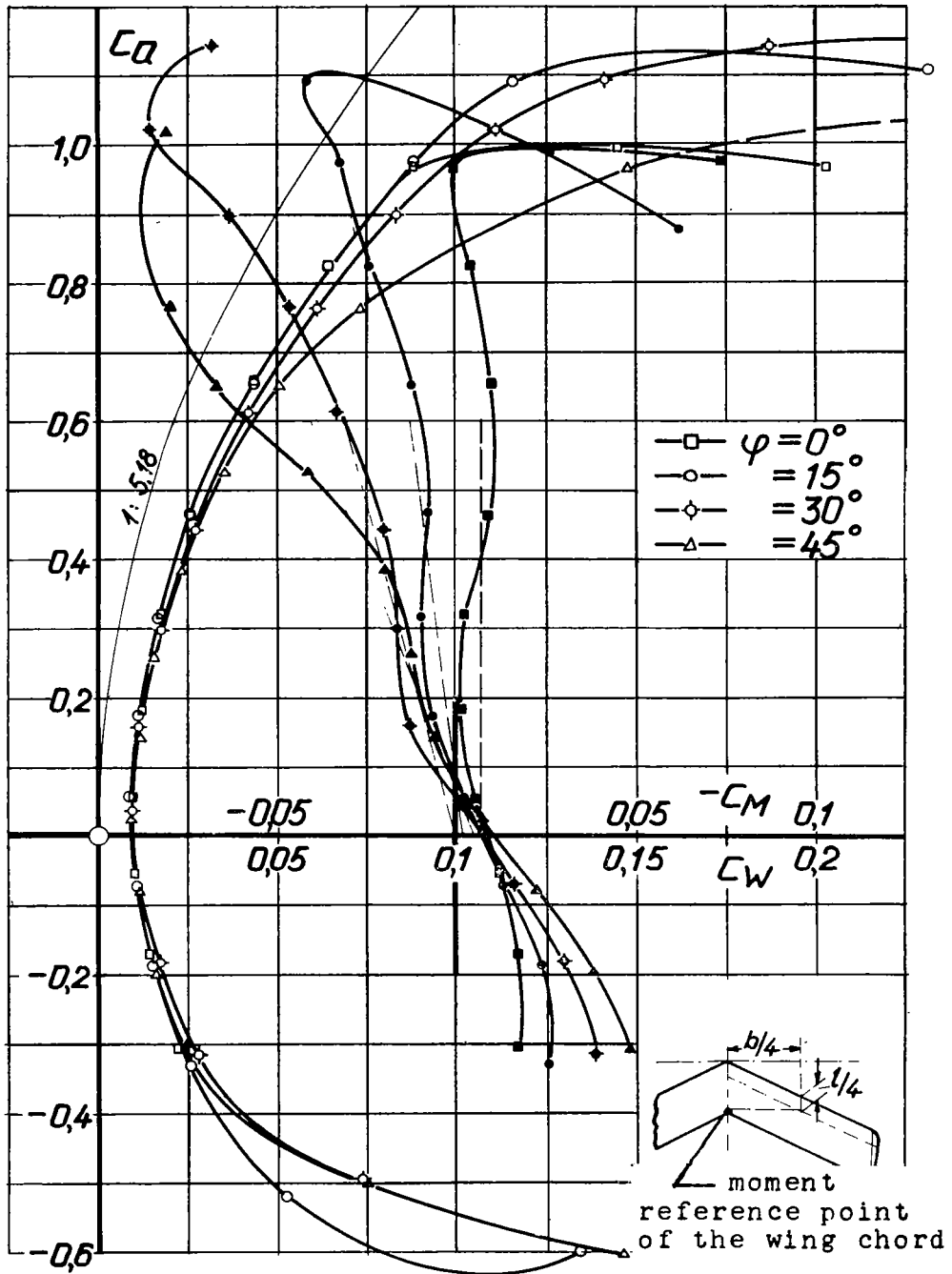


Figure 2.- Polars and moment curves for symmetrical flow.  
 Sweptback angles:  $\psi = 0, 15, 30, 45^\circ$ ;  $\Lambda = 5, 18$ .

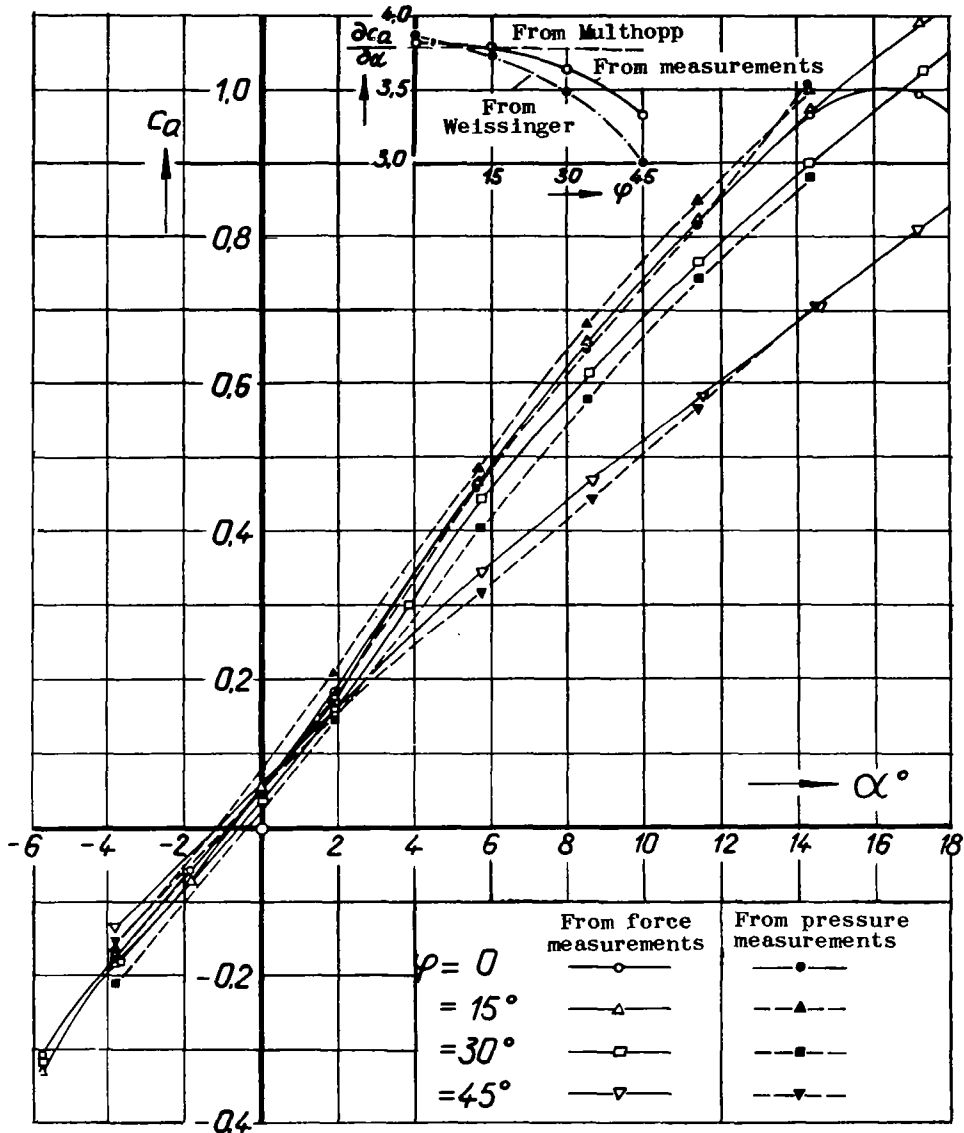
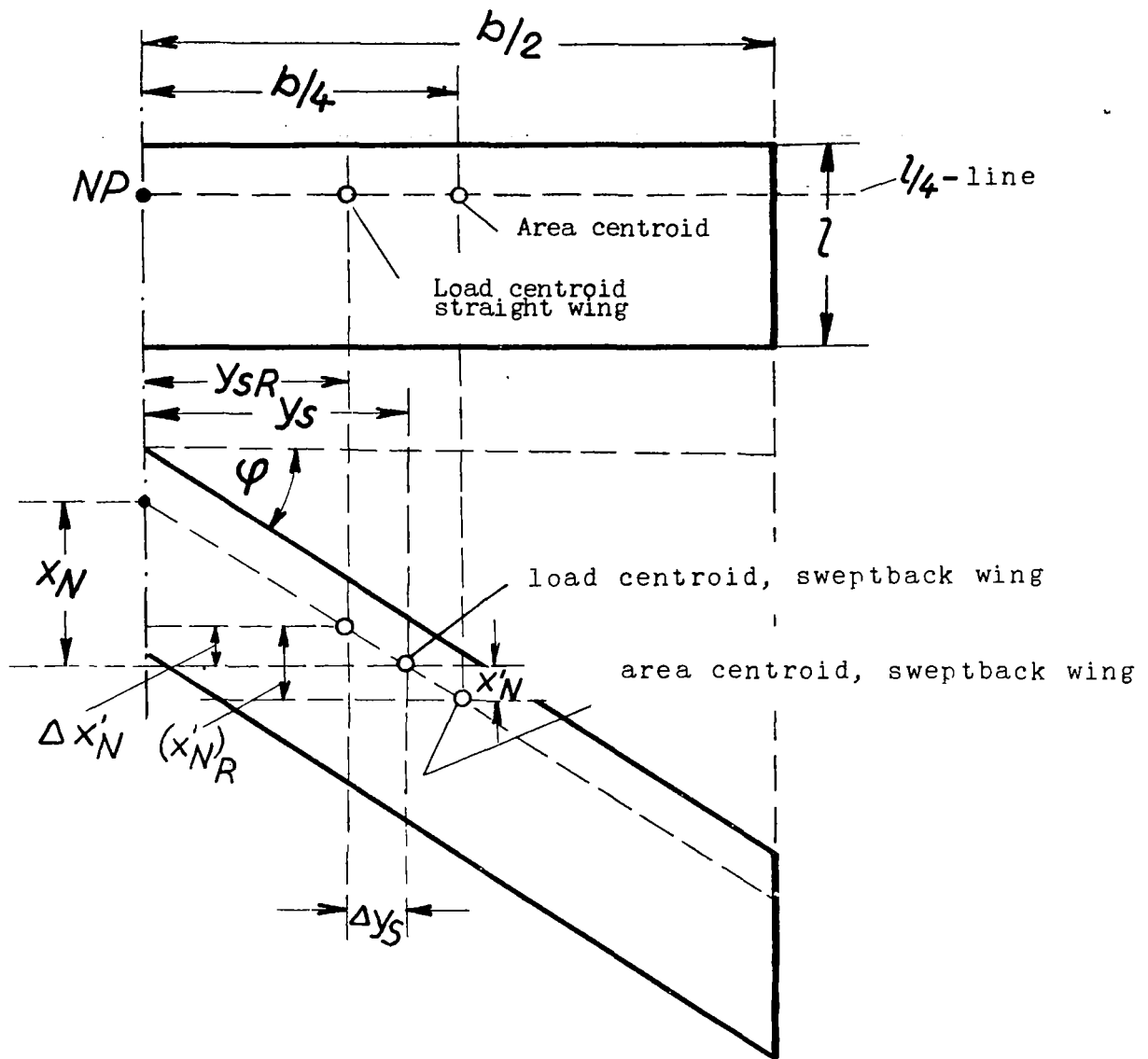


Figure 3.- The relation of lift on angle of attack for symmetrical flow. Comparison between force and pressure measurements. Sweptback wing:  $\phi = 0, 15, 30, 45^\circ$ .



$$\Delta X'_N = (X'_N)_R - X'_N$$

Figure 4. Sketch for the shift in neutral point in the sweptback wing as compared to the straight wing, through shift in load centroid of the lift distribution of a half wing.

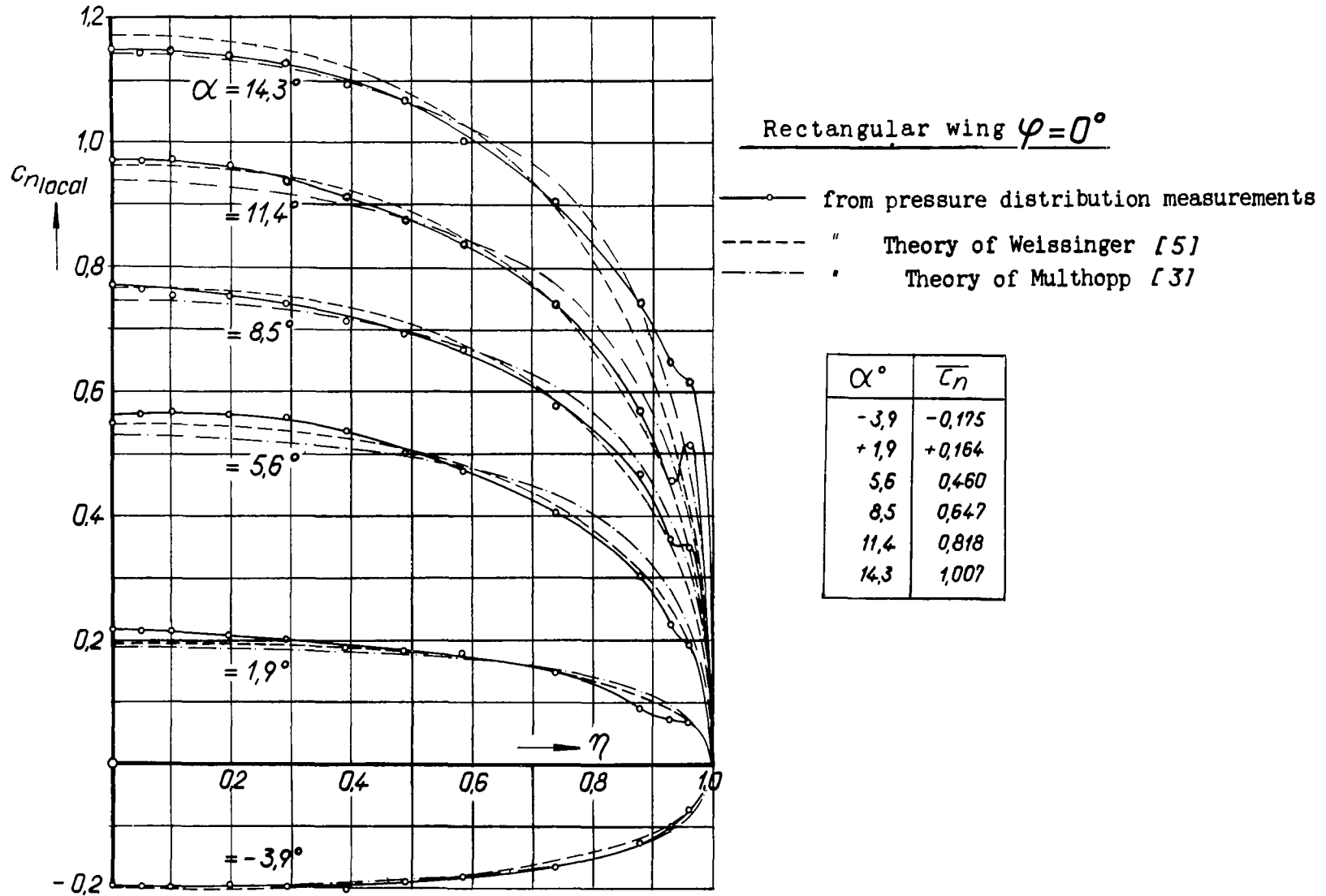
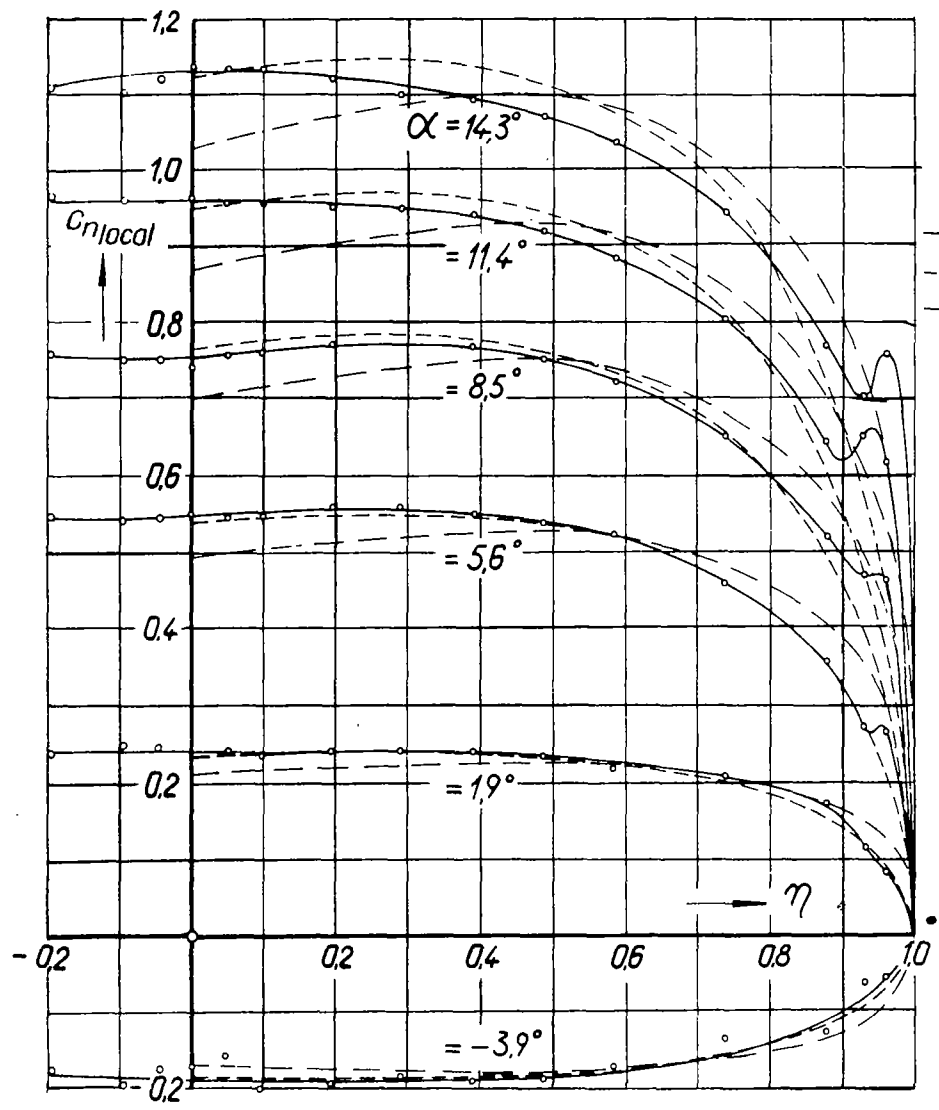


Figure 5. Lift distribution for straight wing,  $\varphi = 0^\circ$  for various angles of attack. comparison of theory and observation.

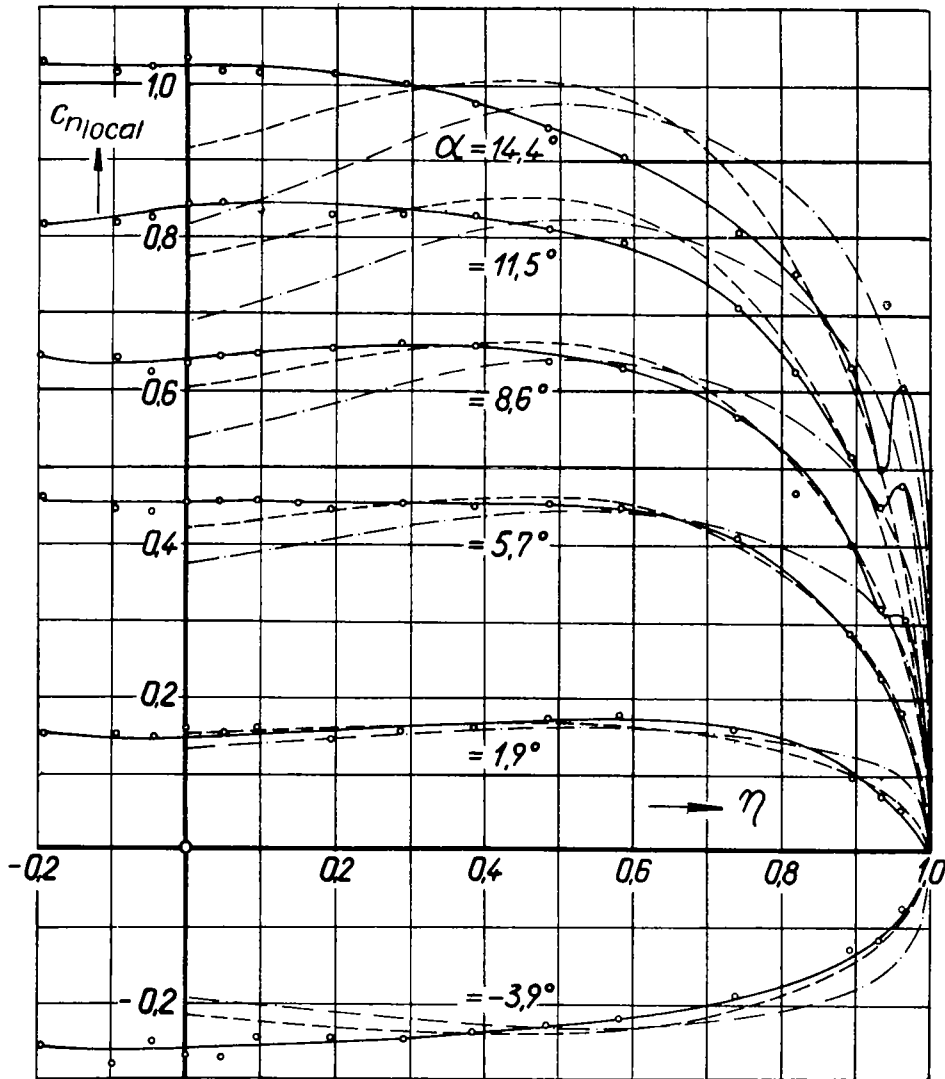


sweptback wing  $\varphi = 15^\circ$

- from pressure distribution measurements
- - - Theory of Weissinger [5]
- · - Theory of Multhopp [3]

$\alpha^\circ$	$\bar{c}_n$
-3.9	-0.163
+1.9	+0.208
5.6	0.483
8.5	0.683
11.4	0.850
14.3	1.001

Figure 6. Lift distribution for sweptback wing,  $\varphi = 15^\circ$  for various angles of attack Comparison of theory and observation.



sweptback wing  $\varphi = 30^\circ$

- from pressure distribution measurements
- - - " Theory of Weissinger [5]
- · - " Theory of Multhopp [3]

$\alpha^\circ$	$\bar{c}_n$
-3,9	-0,210
+1,9	+0,146
5,7	0,405
8,5	0,582
11,4	0,745
14,3	0,882

Figure 7. Lift distribution for sweptback wing,  $\varphi = 30^\circ$  for various angles of attack. Comparison of theory and observation.

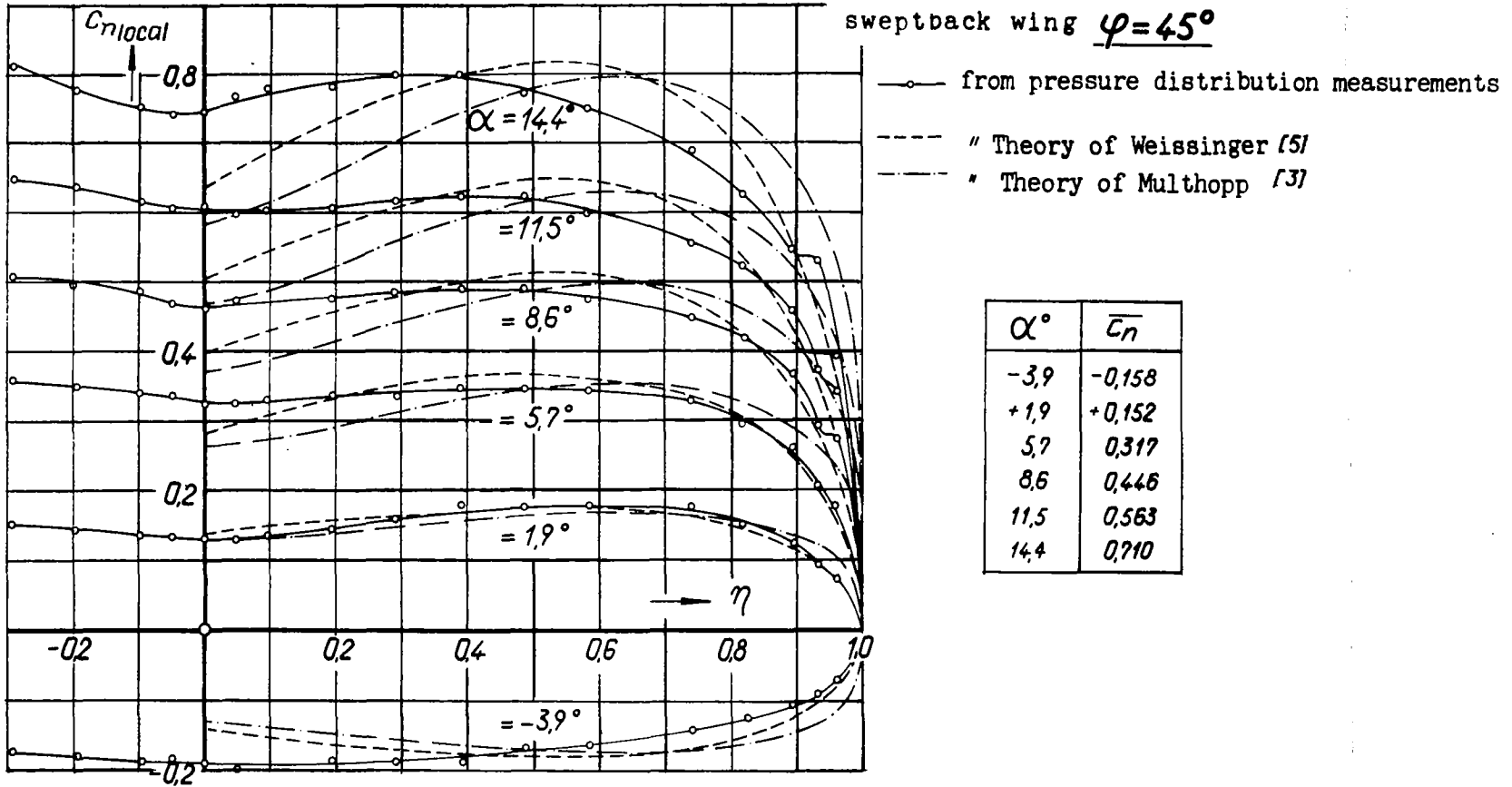
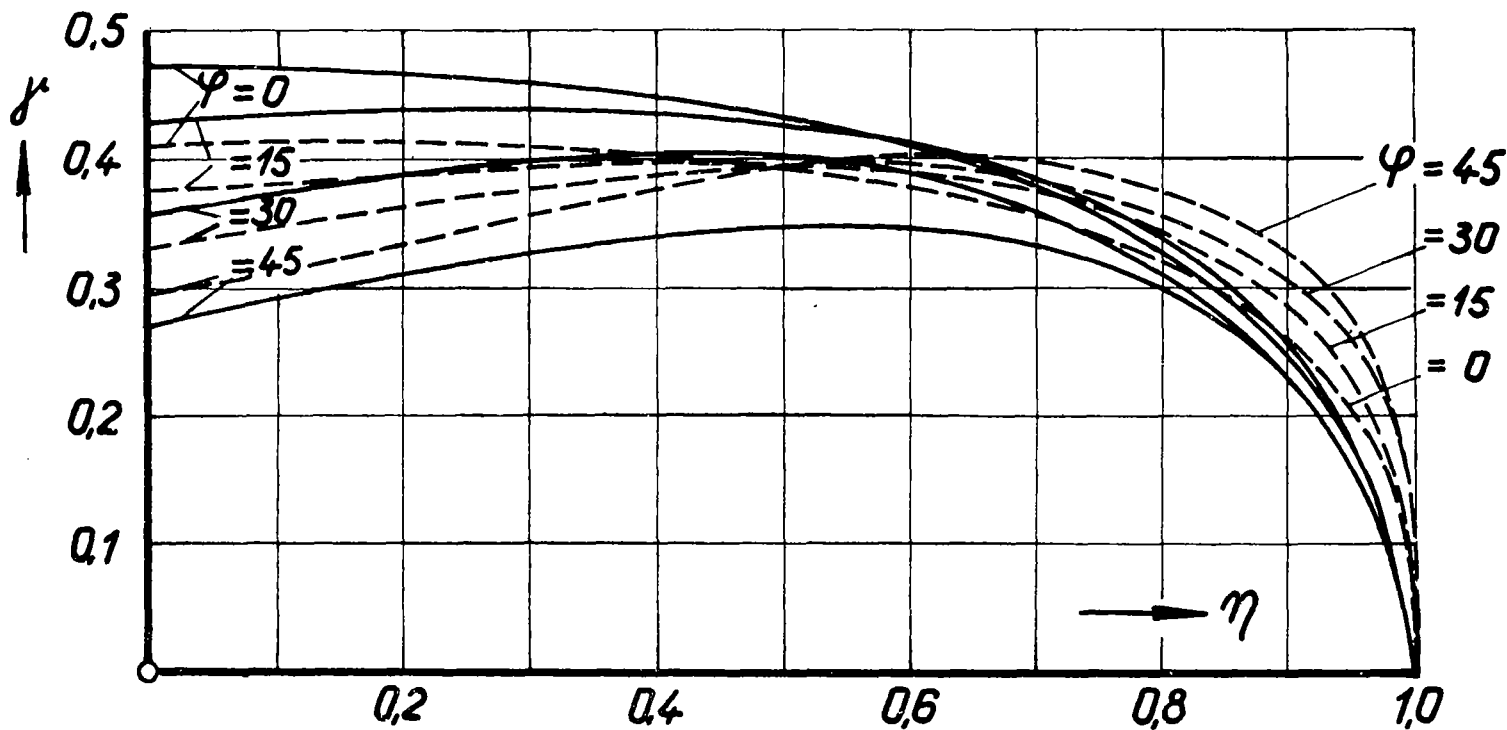


Figure 8. Lift distribution for sweptback wing,  $\varphi = 45^\circ$  for various angles of attack. Comparison of theory and observation.

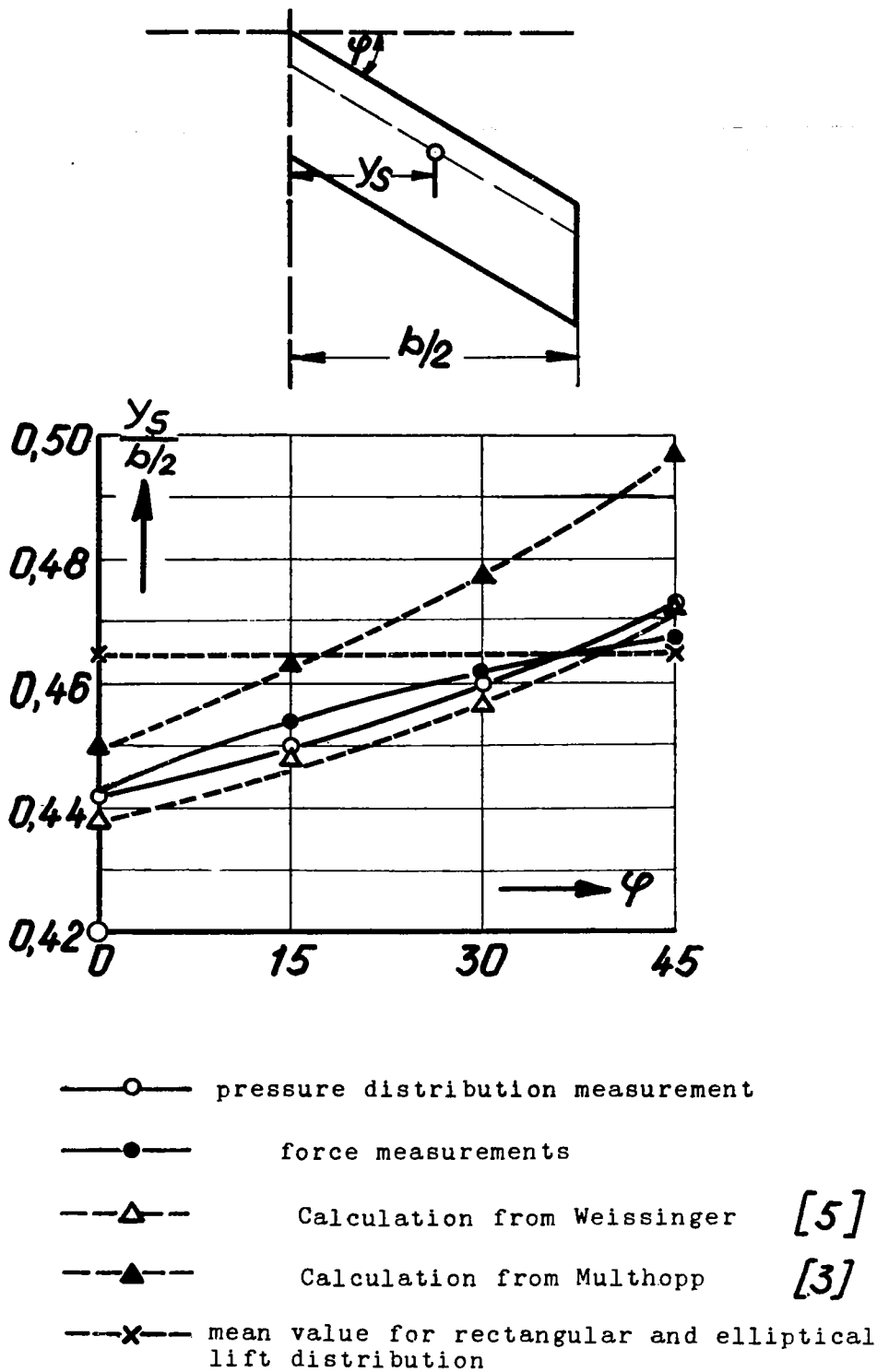
----- from Multhopp's calculation       $\Lambda = 5,18; c_{a\infty} = 5,20; \alpha = 1$   
 \_\_\_\_\_ from Weissinger's calculation       $= 5 ; \quad = 2\pi ; \quad = 1$



The value of  $\partial c_a / \partial \alpha$  :

$\varphi^\circ$	0	15	30	45
Multhopp	3,80	3,80	3,80	3,80
Weissinger	3,89	3,85	3,62	3,33

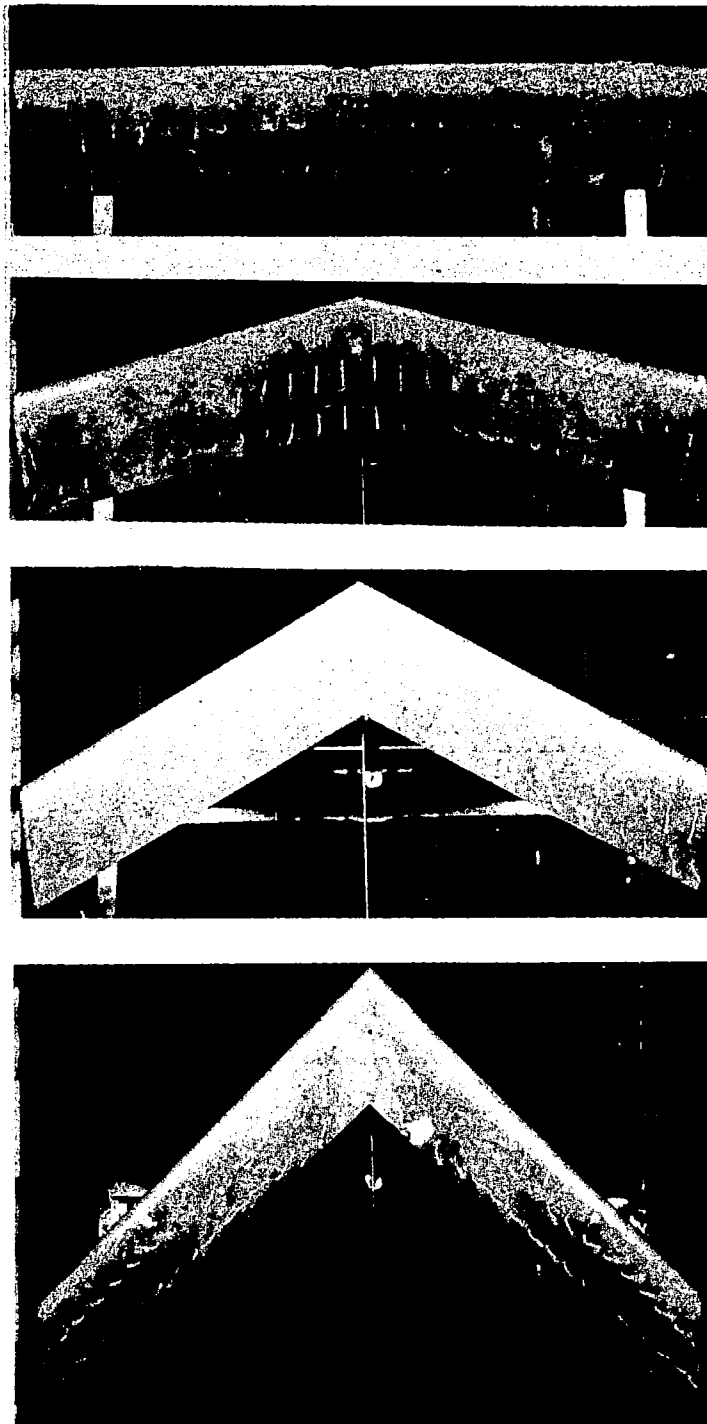
Figure 9. Theoretical lift distributions calculated by Weissinger's and Multhopp's methods.



- pressure distribution measurement
- force measurements
- △--- Calculation from Weissinger [5]
- ▲--- Calculation from Multhopp [3]
- x--- mean value for rectangular and elliptical lift distribution

[1]

Figure 10. Location of the load centroid of the lift distribution of a half-wing as a function of sweepback angle. comparison between theory and observation.



$\varphi =$

$0^\circ$

$15^\circ$

$30^\circ$

$45^\circ$

Figure 11. Flow pictures.

$$\alpha' = 15^\circ \quad \beta = 0$$

NASA Technical Library



3 1176 01441 5559